AMERICAN SOCIETY FOR MICROBIOLOGY | Infection and Immunity®

HOST RESPONSE AND INFLAMMATION

Thioester-Containing Proteins 2 and 4 Affect the Metabolic Activity and Inflammation Response in *Drosophila*

Upasana Shokal,[a] Hannah Kopydlowski,[a] Sneh Harsh,[a] Ioannis Eleftherianos[a]

[a]Infection and Innate Immunity Lab, Department of Biological Sciences, Institute for Biomedical Sciences, The George Washington University, Washington, DC, USA

ABSTRACT *Drosophila melanogaster* is an outstanding model for studying host antipathogen defense. Although substantial progress has been made in understanding how metabolism and immunity are interrelated in flies, little information has been obtained on the molecular players that regulate metabolism and inflammation in *Drosophila* during pathogenic infection. Recently, we reported that the inactivation of thioester-containing protein 2 (*Tep2*) and *Tep4* promotes survival and decreases the bacterial burden in flies upon infection with the virulent pathogens *Photorhabdus luminescens* and *Photorhabdus asymbiotica*. Here, we investigated physiological and pathological defects in *tep* mutant flies in response to *Photorhabdus* challenge. We find that *tep2* and *tep4* loss-of-function mutant flies contain increased levels of carbohydrates and triglycerides in the presence or absence of *Photorhabdus* infection. We also report that *Photorhabdus* infection leads to higher levels of nitric oxide and reduced transcript levels of the apical caspase-encoding gene *Dronc* in *tep2* and *tep4* mutants. We show that *Tep2* and *Tep4* are upregulated mainly in the fat body rather than the gut in *Photorhabdus*-infected wild-type flies and that *tep* mutants contain decreased numbers of *Photorhabdus* bacteria in both tissue types. We propose that the inactivation of *Tep2* or *Tep4* in adult *Drosophila* flies results in lower levels of inflammation and increased energy reserves in response to *Photorhabdus*, which could confer a survival-protective effect during the initial hours of infection.

KEYWORDS *Drosophila*, innate immunity, insect, metabolism, *Photorhabdus*, thioester-containing protein

A central question in insect immunology involves the identification of the pathological defects that lead to insect death following a microbial infection (1). The fruit fly *Drosophila melanogaster* is an established model to interrogate the pathology of infection and inflammation (2–5). *Drosophila* activates distinct immune responses against microbial pathogens. These responses include the activation of NF-κB signaling pathways that lead to the production of antimicrobial peptides and cellular immune reactions that involve phagocytosis, nodulation, and coagulation (6). Infection also induces stress signaling cascades, resulting in the synthesis of nitric oxide (6). To accomplish these immune functions, *Drosophila* relies on its stored reservoirs of energy (7). Metabolism and immunity share a complex relationship depending on the nature of the pathogen that the fly encounters. For example, *Drosophila* flies undergo anorexia after pathogenic infection with *Listeria monocytogenes* and *Salmonella enterica* serovar Typhimurium (8). *L. monocytogenes* infection also depletes the stored energy pools of glycogen and triglycerides, which in turn leads to fly death (9).

The *Drosophila-Photorhabdus* model forms a flexible system for understanding the molecular and mechanistic basis of host-pathogen interactions (10–13). *Photorhabdus* bacteria are Gram-negative bacteria that belong to the family *Enterobacteriaceae*, which

Received 9 November 2017 **Returned for modification** 11 December 2017 **Accepted** 6 February 2018

Accepted manuscript posted online 20 February 2018

Citation Shokal U, Kopydlowski H, Harsh S, Eleftherianos I. 2018. Thioester-containing proteins 2 and 4 affect the metabolic activity and inflammation response in *Drosophila*. Infect Immun 86:e00810-17. https://doi.org/10.1128/IAI.00810-17.

Editor Andreas J. Bäumler, University of California, Davis

Address correspondence to Ioannis Eleftherianos, ioannise@gwu.edu.

includes several other important bacterial pathogens. The main characteristic of *Photorhabdus* is that the bacteria form a mutualistic association with their nematode partner *Heterorhabditis* (14). The bacteria are present in the gut of infective juvenile nematodes that have the ability to attack and invade susceptible insects (15). Following entry, infective juveniles regurgitate *Photorhabdus* in the insect hemocoel, where the bacteria divide exponentially and produce a wide range of toxins and hydrolytic enzymes that cause rapid insect death (16).

The bacteria secrete multiple virulence factors in addition to molecules that interfere with the insect host immune system (17). They can replicate in the insect gut, and as a consequence, the insect ceases feeding and dies due to septicemia (14). *Photorhabdus* also resides and multiplies in insect fat body tissue, an infection strategy that results in the evasion or deactivation of the insect humoral immune response (18). To suppress the cellular immune response, *Photorhabdus* secretes virulence factors that interfere with hemocyte function or morphology, while other secreted molecules promote the death of gut and immune cells (19–21). Although exciting findings have been obtained from studying *Photorhabdus* infection processes in the insect models *Galleria mellonella* and *Manduca sexta* (22–24), the physiological changes caused by these pathogens in *Drosophila* flies have yet to be explored (25).

Thioester-containing proteins (TEPs) participate in the opsonization and elimination of invading microbes in both vertebrate and invertebrate animals, and they are involved in augmenting inflammatory responses in vertebrates (26–28). Substantial information on the function of TEPs in *Anopheles* mosquitoes has been acquired, but only a few studies have examined the contribution of TEPs to the antimicrobial immune response of *Drosophila* (11, 29–34). Recently, we reported that *Tep2*, *Tep4*, and *Tep6* in *Drosophila* are transcriptionally upregulated after infection with *Photorhabdus luminescens* or *Photorhabdus asymbiotica* (11, 35, 36). In particular, the inactivation of *Tep2*, *Tep4*, and *Tep6* in *Drosophila* prolongs the survival of the mutants in response to *Photorhabdus* infection, which is accompanied by a lower level of persistence of the pathogens in infected flies. Here, we have hypothesized that the absence of TEP2 or TEP4 molecules results in lower levels of inflammation in the fly upon *Photorhabdus* infection. For this, we examined the physiological responses of *tep* mutant flies to the two *Photorhabdus* pathogens. We report that *tep2* and *tep4* mutants display increased metabolic reserves and low levels of inflammation in gut and fat body compared to background control flies. Our findings reveal that TEP2 and TEP4 molecules are associated with the regulation of pathophysiological effects, programmed cell death, and metabolic activities in flies in response to *Photorhabdus* challenge.

RESULTS

***Drosophila tep2* mutants exhibit high carbohydrate levels after bacterial infection.** Previous studies have shown that infection with *Listeria monocytogenes* or *Mycobacterium marinum* leads to significant metabolic changes in the fly (9, 37). To understand the prolonged survival of *tep2* and *tep4* mutants, we measured the levels of the carbohydrates trehalose, glycogen, and glucose in flies infected with either pathogenic *Photorhabdus* or nonpathogenic *Escherichia coli* bacteria at early (6 h) and late (18 h) time points postinfection and before fly death occurred (11, 35). We first tested changes in trehalose levels in *tep* mutants and background controls because trehalose is one of the major circulating sugars in fruit flies (38). The levels of trehalose in w^{1118} flies were decreased 6 h after infection with either *Photorhabdus* species and 18 h after infection with *P. luminescens* only compared to phosphate-buffered saline (PBS)-injected controls (Fig. 1A and B). We further observed that *tep2* mutants had significantly higher levels of trehalose than did their background control flies (w^{1118}) 6 h after infection with *E. coli* and *Photorhabdus* (Fig. 1A), whereas no differences were observed between the two mutants 18 h after infection with any of the bacteria or after PBS injection (Fig. 1B). Interestingly, we found no significant changes in trehalose levels between the *tep4* mutants and their background controls (*yw*) at any time point after bacterial infection (Fig. 1C and D). These results demonstrate that the inactivation of *Tep2* affects trehalose

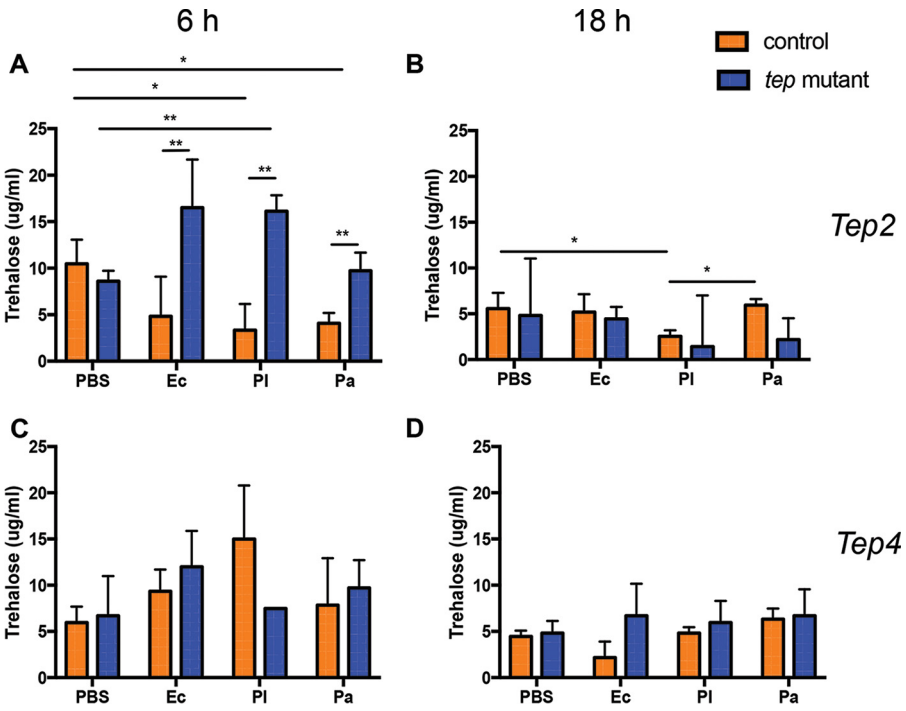

FIG 1 Inactivation of *Tep2* and *Tep4* modulates trehalose levels in *Drosophila* in the presence or absence of *Photorhabdus* infection. Trehalose levels (micrograms per milliliter) in *tep2* (A and B) and *tep4* (C and D) loss-of-function mutants are compared to those in the corresponding background control flies (w^{1118} and *yw*, respectively) ($n = 5$) 6 and 18 h after infection with *E. coli* (Ec), *P. luminescens* (Pl), or *P. asymbiotica* (Pa) or injection with 1× PBS (negative control). The means from three independent experiments are shown, and error bars represent standard deviations. Significant differences are shown with asterisks (*, $P < 0.05$; **, $P < 0.01$).

levels during pathogenic infection with *Photorhabdus* or nonpathogenic infection with *E. coli* bacteria.

Next, we examined the levels of glycogen in *tep* mutants and background controls in the presence or absence of bacterial infection. We found no changes in glycogen levels between the *tep2* mutants and w^{1118} flies at any of the time points (Fig. 2A and B). We also noticed low glycogen levels in w^{1118} flies 6 h after infection with either *Photorhabdus* species and 18 h after infection with *P. luminescens* only compared to the PBS or *E. coli* treatments (Fig. 2A and B). We further observed significantly higher glycogen levels in *tep4* mutants than in their background controls (*yw*) 6 h after infection with *P. luminescens* or *E. coli* or injection with PBS (Fig. 2C and D). In addition, we found that *tep4* mutants had significantly more glycogen than did *yw* flies injected with PBS at 18 h (Fig. 2D). However, *tep4* mutants contained less glycogen 18 h after infection with *P. luminescens* than did those infected with *E. coli* or given control injections with PBS (Fig. 2D). These results indicate that the inactivation of *Tep4* in *Drosophila* affects the utilization of glycogen during the early and late stages of infection with pathogenic and nonpathogenic bacteria.

We next examined the levels of free glucose before and after infection with *E. coli* or *Photorhabdus*. We recorded increased glucose levels in *tep2* mutants compared to w^{1118} flies 18 h after infection with *P. asymbiotica* only (Fig. 3A and B). We also noticed that free glucose levels were decreased in w^{1118} flies 6 h after infection with *E. coli* compared to those in w^{1118} flies injected with PBS (Fig. 3A). There were no changes in free glucose levels between *tep4* mutants and *yw* flies 6 h after the injection of bacteria or PBS (Fig. 3C). In contrast, glucose levels were significantly higher in *tep4* mutant flies injected with *E. coli*, *P. asymbiotica*, or PBS at 18 h than in *yw* flies (Fig. 3D). These results indicate that dysregulation of the expression of *Tep2* results in increased free glucose reserves during *P. asymbiotica* infection, whereas the inactivation of *Tep4* promotes increased free glucose reserves during *E. coli* or *P. asymbiotica* infection.

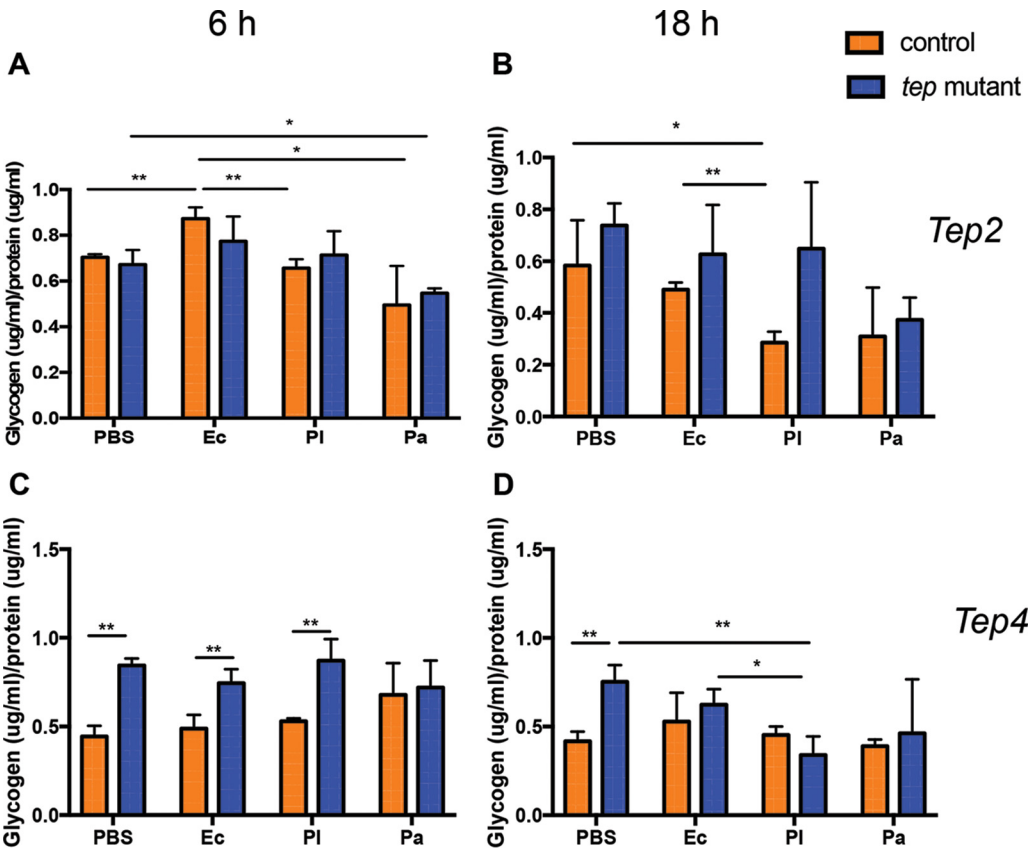

FIG 2 *Drosophila* mutants for *Tep2* and *Tep4* display differential glycogen levels in the presence or absence of *Photorhabdus* infection. Shown are glycogen levels in *tep* loss-of-function mutants and background control flies ($n = 5$) injected with 1× PBS (negative control), *E. coli* (Ec), *P. luminescens* (Pl), or *P. asymbiotica* (Pa). Glycogen levels (micrograms) are normalized to the protein content (micrograms) and represented as a ratio in *tep2* mutants (A and B) and *tep4* mutants (C and D) compared to those of their background control strains (w^{1118} and *yw*, respectively) at 6 and 18 h postinjection. The means from three independent experiments are shown, and error bars represent standard deviations. Significant differences are shown with asterisks (*, $P < 0.05$; **, $P < 0.01$).

***Drosophila tep2* and *tep4* mutants have high triglyceride levels upon bacterial infection.** Previous studies have shown that triglyceride levels decrease with bacterial or viral infection in *Drosophila* (9, 39). Here, we aimed to identify potential changes in triglyceride levels in *tep* mutant flies in response to *Photorhabdus* or *E. coli* infection. We found that *tep2* mutants had higher triglyceride levels than those of the background controls 6 h after infection with *P. asymbiotica* and 18 h after infection with *E. coli* or *Photorhabdus* or injection with PBS (Fig. 4A and B). Similarly, *tep4* mutants displayed increased levels of triglycerides compared to those in *yw* flies with any injection treatment at 6 h postinfection (hpi) but only with PBS or *Photorhabdus* at 18 hpi (Fig. 4C and D). These results imply that the inactivation of *Tep2* or *Tep4* leads to the increased deposition and storage of triglycerides in uninfected or bacterium-infected flies.

***Drosophila tep2* and *tep4* mutants contain large lipid droplets in the fat body after *Photorhabdus* infection.** Previous studies of *Drosophila* identified the participation of lipid droplets (LDs) in the antimicrobial immune response (40, 41). Here, we evaluated the status of LDs localized in the fat body of *tep* mutant flies and background controls in response to pathogenic and nonpathogenic bacterial infections. We observed that uninfected *tep* mutants and their controls displayed similar-sized LDs (Fig. 5A, B, and G and 6A, B, and G). In agreement with the results for triglycerides, we noticed larger LDs in *tep2* and *tep4* mutants after *Photorhabdus* infection than in control flies (Fig. 5C to G and 6C to G). These results indicate that the inactivation of *Tep2* or

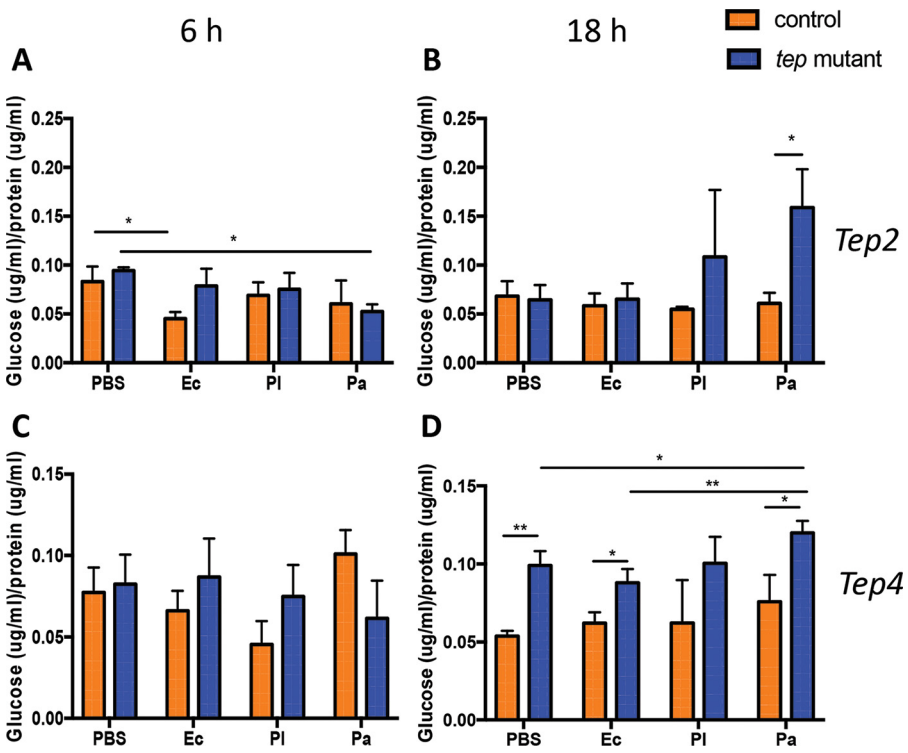

FIG 3 *Drosophila* mutants for *Tep2* and *Tep4* have altered glucose levels upon infection with *Photorhabdus*. Shown are free glucose levels in *tep2* (A and B) and *tep4* (C and D) loss-of-function mutant flies compared to those in the corresponding background controls (w^{1118} and *yw*, respectively) ($n = 5$) 6 and 18 h after infection with *E. coli* (Ec), *P. luminescens* (Pl), or *P. asymbiotica* (Pa) or injection with 1× PBS (negative control). Glucose levels are normalized to the total protein content and represented as a ratio of the total glucose content to the total protein content. The means from three independent experiments are shown, and error bars represent standard deviations. Significant differences are shown with asterisks (*, $P < 0.05$; **, $P < 0.01$).

Tep4 regulates the size of LDs in the fat body of flies in response to *Photorhabdus* infection.

***Drosophila tep2* and *tep4* mutants contain fewer *Photorhabdus* cells in gut and fat body.** Previously, we reported a lower level of persistence of *Photorhabdus* in *tep2* and *tep4* mutant flies (11, 35). Here, we estimated the number of bacteria in the gut and fat body of *tep* mutants 18 h after infection with *E. coli* and *Photorhabdus*. We found higher numbers of *Photorhabdus* CFU in the fat body than in the gut in all four fly strains (Fig. 7). However, there were no changes in *P. luminescens* burdens between *tep2* and control flies in either the fat body or gut (Fig. 7A). Instead, there were significantly fewer *P. asymbiotica* CFU in the gut of *tep2* mutants than in control flies (Fig. 7B). Similar to our previously reported results (11), we observed significantly fewer CFU of *P. luminescens* in both tissues of *tep4* mutants than in the tissues of control flies, whereas there was no difference in *P. asymbiotica* CFU between the two strains (Fig. 7C and D). We were unable to detect the presence of *E. coli* in either tissue of *tep* mutants and their background controls by quantitative PCR (qPCR) at 18 hpi. These results suggest that the inactivation of *Tep2* or *Tep4* regulates *Photorhabdus* replication in the fly gut and fat body during early and late hours of infection.

***Photorhabdus* infection increases *Tep2* and *Tep4* transcript levels in the fly gut and fat body.** *Tep* genes are induced in the larval fat body and in the abdominal epithelium of the gut in the adult fly (31). We recently found increased transcript levels of *Tep2* and *Tep4* in *yw* and w^{1118} background fly strains upon *E. coli* or *Photorhabdus* infection (11, 35). Therefore, we investigated whether *Tep2* and *Tep4* are expressed mainly in the gut and fat body of background control flies 18 h after infection with these bacteria. We found that *Tep2* was upregulated in the fly fat body upon infection

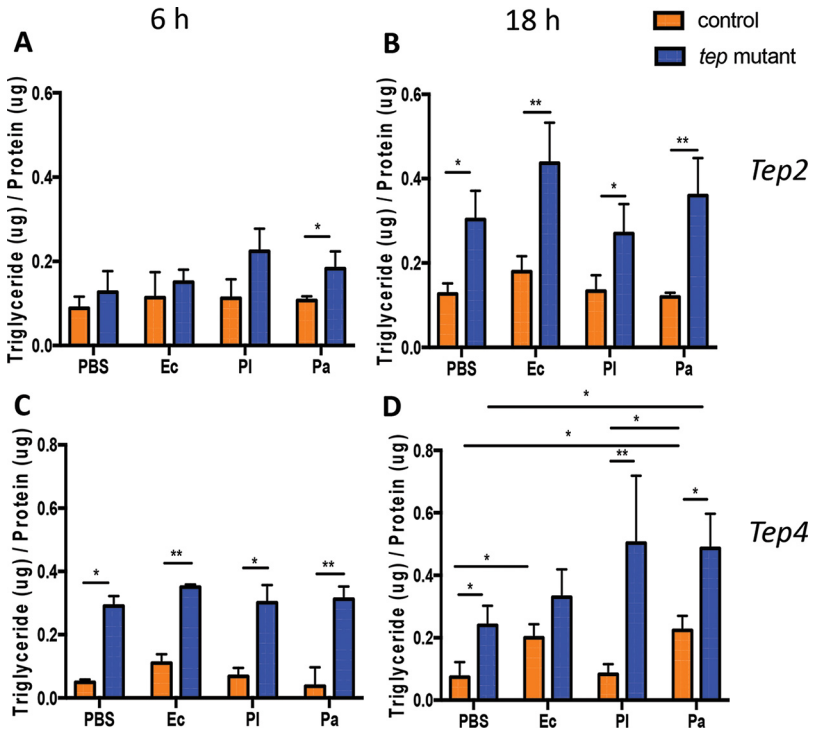

FIG 4 Infection of *Drosophila tep2* and *tep4* mutant flies with *Photorhabdus* alters triglyceride levels. Shown are estimations of triglyceride levels in *tep* loss-of-function mutants and background controls ($n = 5$) injected with 1× PBS (negative control), *E. coli* (Ec), *P. luminescens* (Pl), or *P. asymbiotica* (Pa). Triglyceride levels (micrograms) are normalized to the protein content (micrograms) and represented as a ratio of the total triglyceride content to the total protein content in *tep2* mutants (A and B) and *tep4* mutants (C and D) compared to the background control strains (w^{1118} and *yw*, respectively) at 6 and 18 h postinfection. The means from three independent experiments are shown, and error bars represent standard deviations. Significant differences are shown with asterisks (*, $P < 0.05$; **, $P < 0.01$).

with *P. luminescens* only, whereas infection with this pathogen induced *Tep4* in both tissues (Fig. 7F). In addition, *Tep4* was upregulated in the fat body of *P. asymbiotica*-infected flies (Fig. 7F). These results indicate that the *Drosophila* gut is a source of *Tep2* expression, whereas both gut and fat body tissues are involved in the induction of *Tep4* expression in adult flies in response to *Photorhabdus* infection.

***Drosophila tep2* and *tep4* mutants have high nitric oxide activity in response to bacterial infection.** Because *tep* mutants contain larger amounts of sugars and triglycerides but lower bacterial burdens in the fat body and gut, we measured stress levels in these flies upon *Photorhabdus* or *E. coli* infection. For this, we estimated the levels of nitrite, a by-product of nitric oxide production that is used as a measure of stress in insects (42). We found that *tep2* mutants had significantly lower nitrite levels than those of w^{1118} flies 6 h after infection with *P. luminescens* (Fig. 8A) but significantly higher nitrite levels 18 h after infection with *E. coli* or *Photorhabdus* than those of their counterparts injected with PBS (Fig. 8B). Similarly, w^{1118} flies had higher nitrite levels 18 h after infection with *Photorhabdus* than those of *E. coli*-infected or PBS-injected individuals (Fig. 8B). In *tep4* mutants, there was a decrease in the nitrite quantity 6 h after infection with *Photorhabdus* or *E. coli* compared to that in PBS-injected flies (Fig. 8C). However, *yw* flies injected with *P. luminescens* had significantly increased nitrite levels compared to those in *yw* flies injected with *E. coli* or PBS at 18 hpi (Fig. 8D). We also found higher nitrite levels in *tep4* mutant flies injected with *P. asymbiotica* than in those injected with PBS, *E. coli*, or *P. luminescens* at 18 hpi (Fig. 8D). Finally, *tep4* mutants contained large amounts of nitrite after injection with PBS, *E. coli*, or *P. luminescens* at 6 and 18 hpi compared to those in *yw* background flies (Fig. 8C and D). These results indicate that flies with inactivated *Tep4* have increased stress levels in response to *Photorhabdus* or *E. coli* infection.

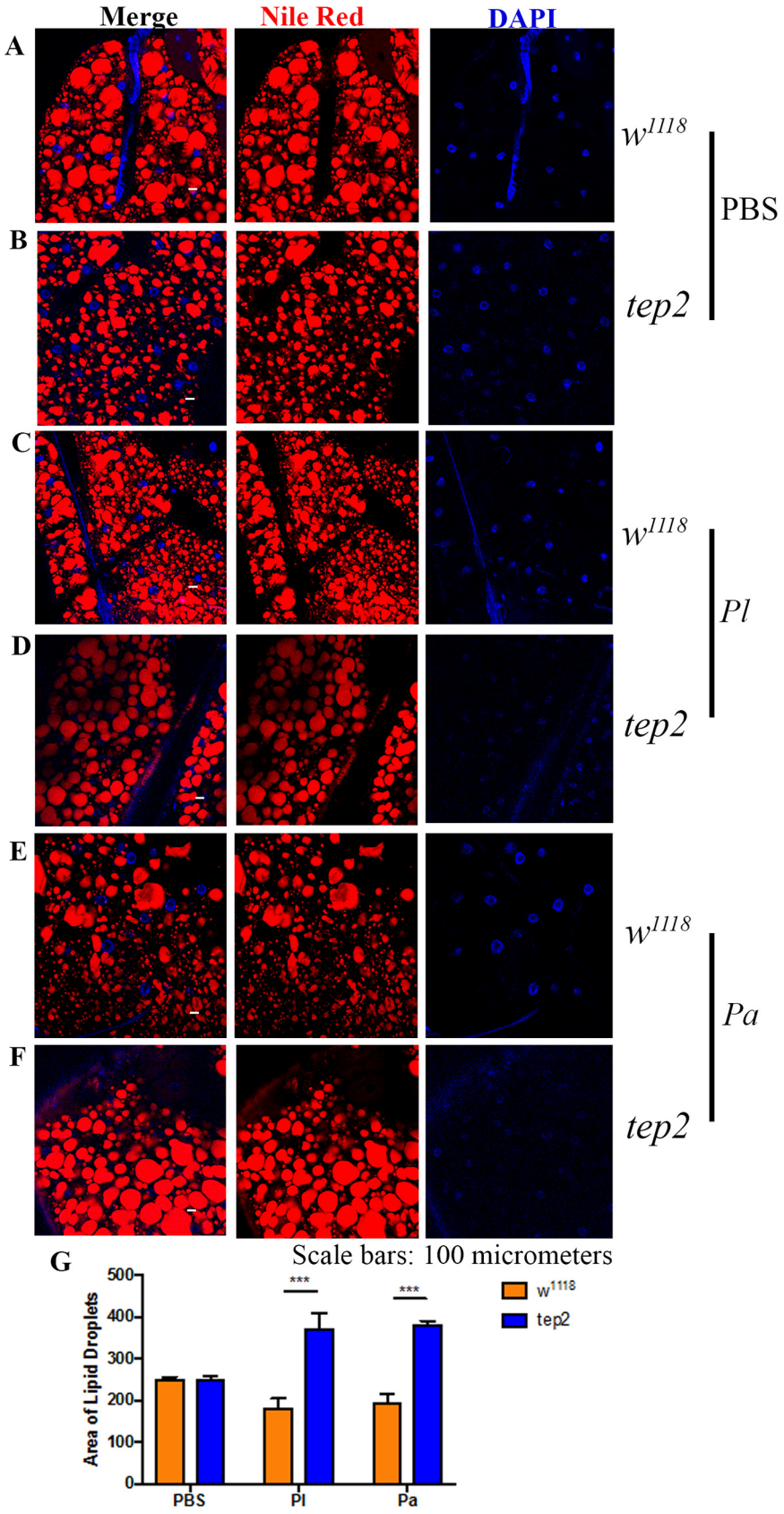

FIG 5 *Drosophila* mutants for *Tep2* display large lipid droplets after *Photorhabdus* infection. (A to F) Fat body tissues were stained with Nile Red-O as well as DAPI (4′,6-diamidino-2-phenylindole) and observed

(Continued on next page)

***Drosophila tep2* and *tep4* mutants undergo reduced cell death upon infection with *Photorhabdus*.** To investigate whether the prolonged-survival phenotype of *tep* mutants in response to *Photorhabdus* infection is due to reduced apoptotic death (11), we examined the transcript levels of *Dronc*, an ortholog of mammalian caspase-9 (43). The initiator (apical) caspase DRONC is required for the induction of apoptosis in flies (44). We found that w^{1118} flies had increased *Dronc* transcript levels 6 h after infection with *E. coli* or injection with PBS compared to those in *tep2* mutants (Fig. 9A). Eighteen hours after infection with *P. asymbiotica*, w^{1118} flies displayed increased transcript levels of *Dronc* compared to those in *tep2* mutants and w^{1118} flies infected with *E. coli* or injected with PBS (Fig. 9B). Moreover, *tep2* mutants had significantly higher *Dronc* transcript levels after *P. luminescens* infection than did those injected with *E. coli* or PBS (Fig. 9B). *yw* flies had increased transcript levels of *Dronc* 18 h after infection with *P. luminescens* compared to those in flies injected with *P. asymbiotica*, *E. coli*, or PBS (Fig. 9C and D). For *tep4* mutants, we observed lower *Dronc* transcript levels than those in *yw* flies 18 h after infection with *P. luminescens* (Fig. 9C and D). In addition, *Dronc* transcript levels in *tep4* mutants 18 h after infection with *P. luminescens* were high in *tep4* mutants compared to those in flies infected with *P. asymbiotica* or injected with PBS (Fig. 9D). These findings suggest that the inactivation of *Tep2* or *Tep4* is linked to reduced cell death in *Photorhabdus*-infected flies, which is probably due to a lower level of persistence of the pathogens.

To investigate cell death at the tissue level, we also estimated the expression level of the death caspase-1 (DCP-1) protein in the midgut of *tep2* and *tep4* mutants as well as in the corresponding background control flies. We chose the midgut for these experiments because *Photorhabdus* damages this tissue by inducing cell death (17). We were not able to identify changes in DCP-1 expression between *tep2* mutants and control flies injected with PBS (Fig. 10A and B). However, we found lower DCP-1 expression levels in *tep2* mutants than in w^{1118} flies infected with *Photorhabdus* bacteria at 18 hpi (Fig. 10C to G). Similarly, there were no changes in DCP-1 expression levels between *tep4* mutants and *yw* flies injected with PBS (Fig. 11A and B). Finally, we found that *tep4* mutants had lower expression levels of DCP-1 than did *yw* flies 18 h after infection with *Photorhabdus* (Fig. 11C to G). These results indicate that the inactivation of *Tep2* or *Tep4* results in decreased expression levels of caspases in flies infected with *Photorhabdus* pathogens.

DISCUSSION

In this study, we investigated the pathological defects in *tep* loss-of-function mutant flies in response to *Photorhabdus* infection. We evaluated the amounts of different metabolites, such as carbohydrates and lipids, to monitor metabolic activity in the presence or absence *Photorhabdus* infection. We also examined the levels of stress, cell death, and pathogen burden in *tep* mutant flies as indicators of inflammation upon infection with these pathogens. We report that the inactivation of *Tep2* or *Tep4* results in increased physiological responses and reduced inflammation in flies infected with *Photorhabdus* bacteria.

Metabolic changes in the whole animal reflect changes that take place at the physiological or immunological level (45). Hence, by examining physiological activities in infected *tep* mutants, we aimed to understand the cause(s) for their altered survival response to *Photorhabdus* (11). Previously, we showed that TEP2 and TEP4 are involved in regulating the activation of immune signaling pathways in *Photorhabdus*-infected

FIG 5 Legend (Continued)
under a confocal microscope (Olympus) at a ×20 magnification. Lipid droplets (red) and nuclei (blue) are shown for flies of the background control strain (w^{1118}) (A, C, and E) and the *tep2* mutant strain (B, D, and F) 18 h after infection with *Photorhabdus luminescens* (Pl) or *P. asymbiotica* (Pa) or injection with 1× PBS (negative control). (G) Areas of lipid droplets in fat body cells of the background control strain (w^{1118}) as well as *tep2* mutants were quantified by using ImageJ. The means from at least three independent fat body samples are shown, and error bars represent standard deviations. Significant differences are shown with asterisks (***, $P < 0.001$).

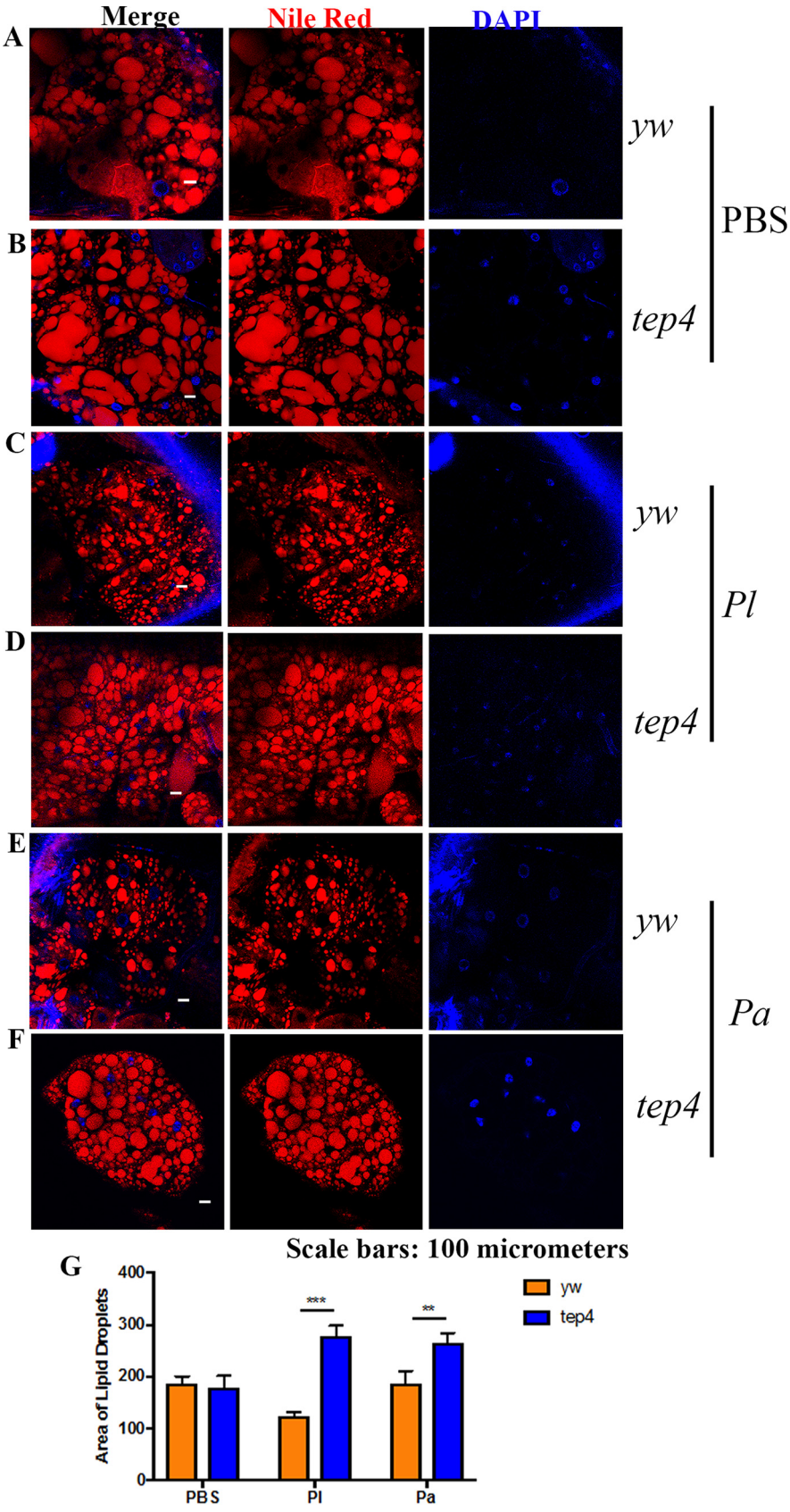

FIG 6 *Drosophila* mutants for *Tep4* display large lipid droplets after *Photorhabdus* infection. (A to F) Fat body tissues were stained with Nile Red-O as well as DAPI and observed under a confocal microscope

(Continued on next page)

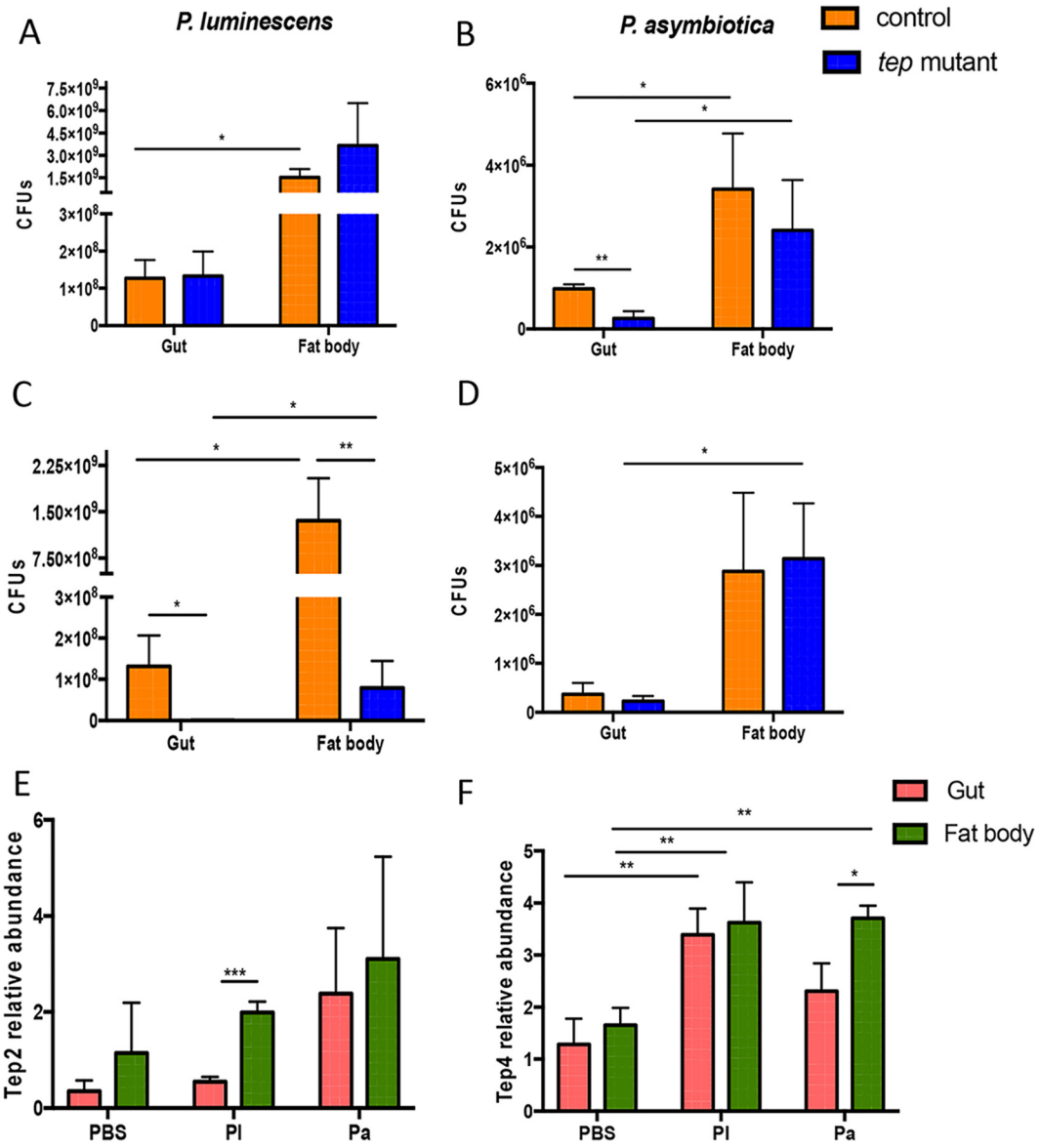

FIG 7 Pathogen burden and *Tep* gene transcript levels are altered in the gut and fat body of *Drosophila* flies in response to *Photorhabdus* infection. (A to D) CFU of *P. luminescens* (A and C) and *P. asymbiotica* (B and D) in the gut and fat body of *tep2* and *tep4* mutant flies and background control flies (w^{1118} and *yw*, respectively) ($n = 5$ per experimental condition) at 18 h postinfection. CFU were estimated by quantitative PCR of *Photorhabdus* 16S rRNA levels. (E and F) Transcript levels of *Tep2* (E) and *Tep4* (F) in the gut and fat body tissues of w^{1118} flies ($n = 5$) 18 h after infection with *E. coli* (Ec), *P. luminescens* (Pl), or *P. asymbiotica* (Pa) or injection with 1× PBS (negative control). Gene transcript levels are shown as relative abundances of transcripts normalized to the value for the ribosomal protein L32 gene (*RpL32*) and expressed as a ratio compared to values for uninfected flies. The means from three independent experiments are shown, and error bars represent standard deviations. Significant differences are indicated with asterisks (*, $P < 0.05$; **, $P < 0.01$; ***, $P < 0.001$).

flies (11, 35). Several studies have linked immune signaling pathway activity to metabolic status in *Drosophila* in the context of infection (7). For example, insulin signaling and triglyceride synthesis were attenuated in *Toll* gain-of-function mutants, but not in *Imd* mutants, in the absence of infection (46). The induction of the Toll pathway by

FIG 6 Legend (Continued)
(Olympus) at a ×20 magnification. Lipid droplets (red) and nuclei (blue) are shown for flies of the background control strain (*yw*) (A, C, and E) and the *tep4* strain (B, D, and F) 18 h after infection with *Photorhabdus luminescens* (Pl) or *P. asymbiotica* (Pa) or injection with 1× PBS (negative control). (G) Areas of lipid droplets in fat body cells of the background control strain (*yw*) as well as *tep4* mutants were quantified by using ImageJ. The means from three independent fat body samples are shown, and error bars represent standard deviations. Significant differences are shown with asterisks (**, $P < 0.01$; ***, $P < 0.001$).

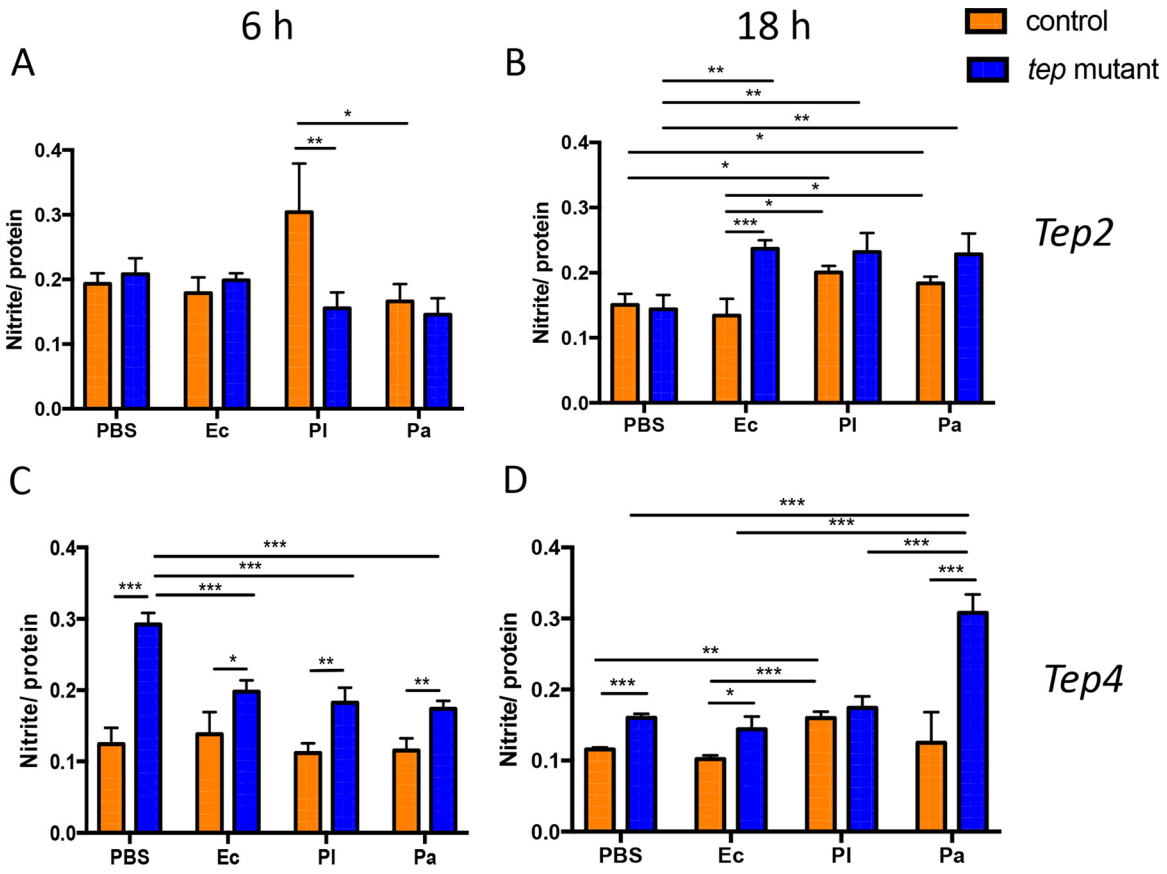

FIG 8 *Drosophila* mutants for *Tep2* and *Tep4* exhibit elevated levels of nitric oxide after infection with *Photorhabdus*. Nitrite levels in *tep* loss-of-function mutants and background controls ($n = 5$) injected with *E. coli* (Ec), *P. luminescens* (PI), *P. asymbiotica* (Pa), or 1× PBS (negative control) were estimated. The concentration of nitrite (micromolar) is normalized to the protein content (micrograms per milliliter) and represented as a ratio of total nitrite levels to total protein levels in *tep2* mutants (A and B) and *tep4* mutants (C and D) with the corresponding background control strains (w^{1118} and *yw*, respectively) at 6 and 18 h postinjection. The means from three independent experiments are shown, and error bars represent standard deviations. Significant differences are shown with asterisks (*, $P < 0.05$; **, $P < 0.01$; ***, $P < 0.001$).

bacterial infection results in a reduction of insulin signaling. In addition, the Imd pathway negatively modulates certain metabolic genes in response to Gram-negative bacterial infection in fruit flies (47). Therefore, we propose that the increased levels of carbohydrates and triglycerides in *tep* mutants compared to those in the background control flies could be the result of an indirect attenuation of insulin signaling due to differential regulation of immune signaling in the absence of functional TEP molecules. Moreover, the decreased levels of trehalose and glycogen in *tep2* and *tep4* mutants, respectively, during the late stages of *Photorhabdus* infection may be the result of using up the stored energy in these flies. Once these energy reservoirs are exhausted, the synthesis of various metabolites, such as proteins, lipids, and carbohydrates, in response to bacterial infection might cease in *tep* mutant flies (48).

Lipid droplets are multifunctional organs present in most organisms ranging from bacteria to eukaryotes. They are abundantly present in fat-storing tissues, such as insect fat body cells. Lipid droplets perform immune activities in mammals, mosquitoes, and *Drosophila* (40, 49, 50). Interestingly, lipid droplets have been shown to accumulate in neutrophils and macrophages during infection in mammals (50). Moreover, the constitutive activation of Toll and Imd pathways in *Aedes* mosquitoes leads to the accumulation of lipid droplets in the midgut (40, 49). Therefore, our present findings indicate that the induction of Toll and Imd signaling in flies with inactivated *tep* genes could be linked to changes in the numbers of lipid droplets in the context of *Photorhabdus* infection. The exact mechanism of this physiological alteration requires further investigation and will form the basis of our future studies.

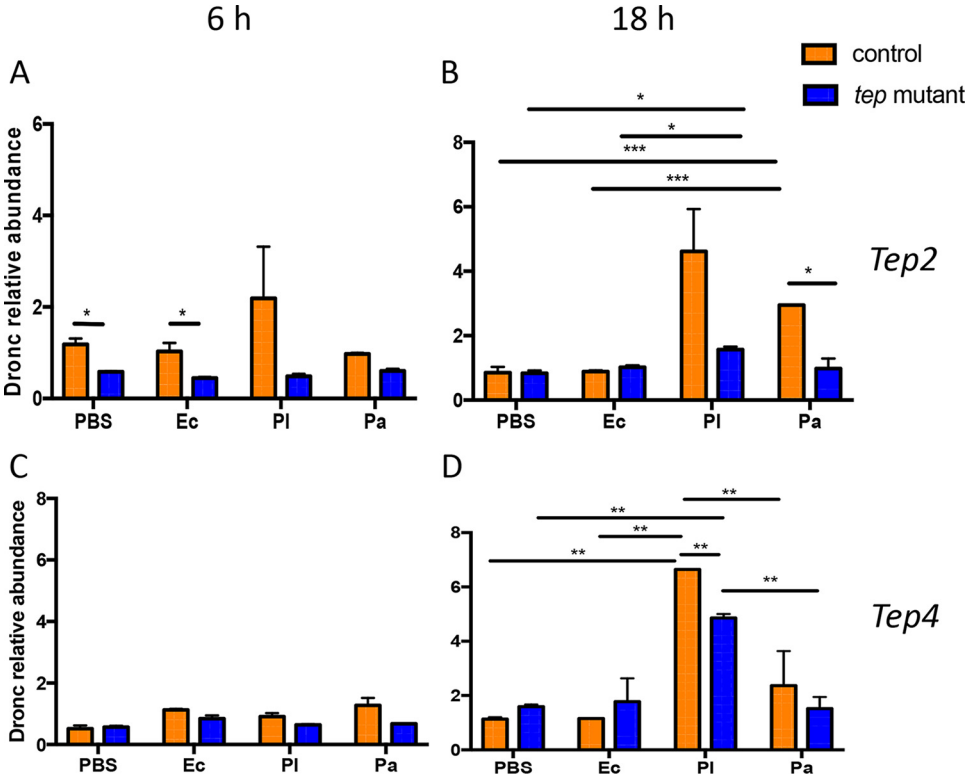

FIG 9 *Drosophila* mutants for *Tep2* and *Tep4* have reduced apoptosis upon *Photorhabdus* infection. Shown are transcript levels of *Dronc* in *tep2* (A and B) and *tep4* (C and D) mutant flies compared to the corresponding background controls (w^{1118} and *yw*, respectively; $n = 3$ to 5) 6 and 18 h after infection with *E. coli* (Ec), *P. luminescens* (Pl), or *P. asymbiotica* (Pa) or injection with 1× PBS (negative control). Gene transcript levels are shown as relative abundances of transcripts normalized to the value for the ribosomal protein L32 housekeeping gene (*RpL32*) and expressed as a ratio compared to the values for uninfected flies. The means from three independent experiments are shown, and error bars represent standard deviations. Significant differences are indicated with asterisks (*, $P < 0.05$; **, $P < 0.01$; ***, $P < 0.001$).

The fat body and gut tissues of *Drosophila* are the sites of systemic and local antimicrobial peptide synthesis, respectively (51, 52). *Tep* genes are upregulated in the abdominal epithelium and larval fat body upon septic injury (31), and our results are in accordance, as we report the induction of *Tep2* and *Tep4* in the fat body as well as the gut after *Photorhabdus* infection. During *Photorhabdus* infection, the bacteria first grow excessively in the insect hemolymph and gut and subsequently proliferate in the fat body (14, 18). The increased colonization of *Photorhabdus* in the fat body at late time points suggests that this tissue might form the main target for these pathogens, which could lead to the suppression of the humoral immune response (53). In addition, the presence of *Photorhabdus* in the gut could also form an evasion strategy for direct interference with the gut epithelial immune response (17). Interestingly, the level of persistence of *Photorhabdus* in *tep* mutants is consistently low, which implies that there is a potential interaction of TEP molecules with the pathogens. We propose that this interaction might promote *Photorhabdus* pathogenicity, which could lead to the depletion of energy stores and, ultimately, the death of the fly.

Nitric oxide signaling is known to activate the innate immune response in *Drosophila* upon infection with Gram-negative bacteria (6, 54). Nitric oxide synthase provides protection against *Photorhabdus* infection in *Manduca sexta* and *Drosophila* and can increase melanization and clot formation (55, 56). Increased nitric oxide levels in uninfected and infected *tep* mutants could potentially activate humoral immune responses early in an infection by *Photorhabdus*. Therefore, we propose that the inactivation of *Tep2* or *Tep4* interferes with nitric oxide activity that could stimulate immune signaling pathways in the fly (35, 36). Consequently, this would result in

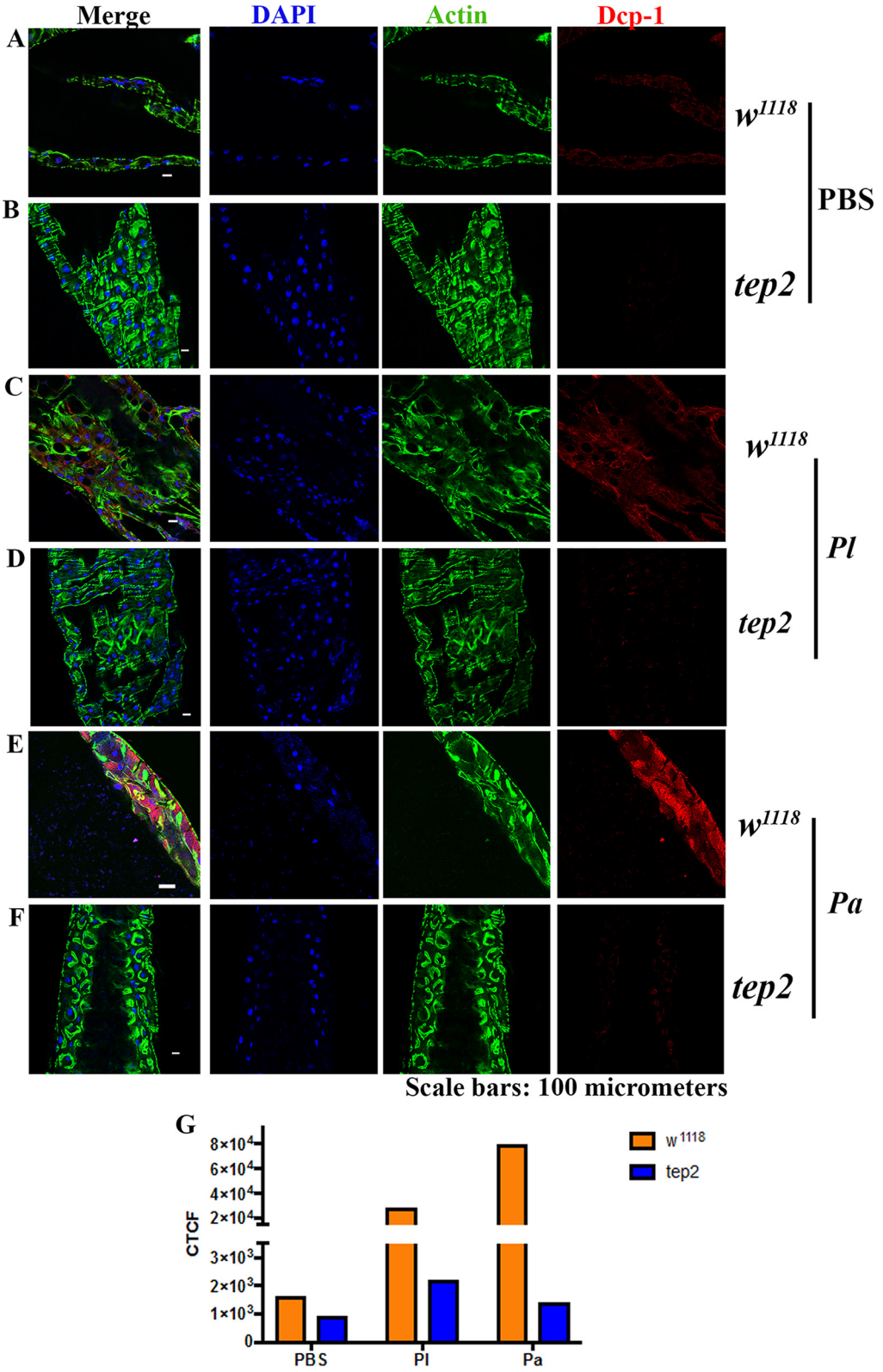

FIG 10 *Drosophila* mutants for *Tep2* show low DCP-1 expression levels in the midgut following infection with *P. luminescens*. (A to F) Guts from 7- to 10-day-old *tep2* mutants and background control flies (w^{1118}) were stained with DCP-1 (red), DAPI (blue), and phalloidin (green). The dissected, stained tissues of flies injected with 1× PBS (A and B), *P. luminescens* (Pl) (C and D), and *P. asymbiotica* (Pa) (E and F) were observed at a ×40 magnification under a confocal microscope. (G) Corrected total cell fluorescence (CTCF) was measured to quantify the expression level of DCP-1 in both background control flies (w^{1118}) and *tep2* mutant flies by using ImageJ.

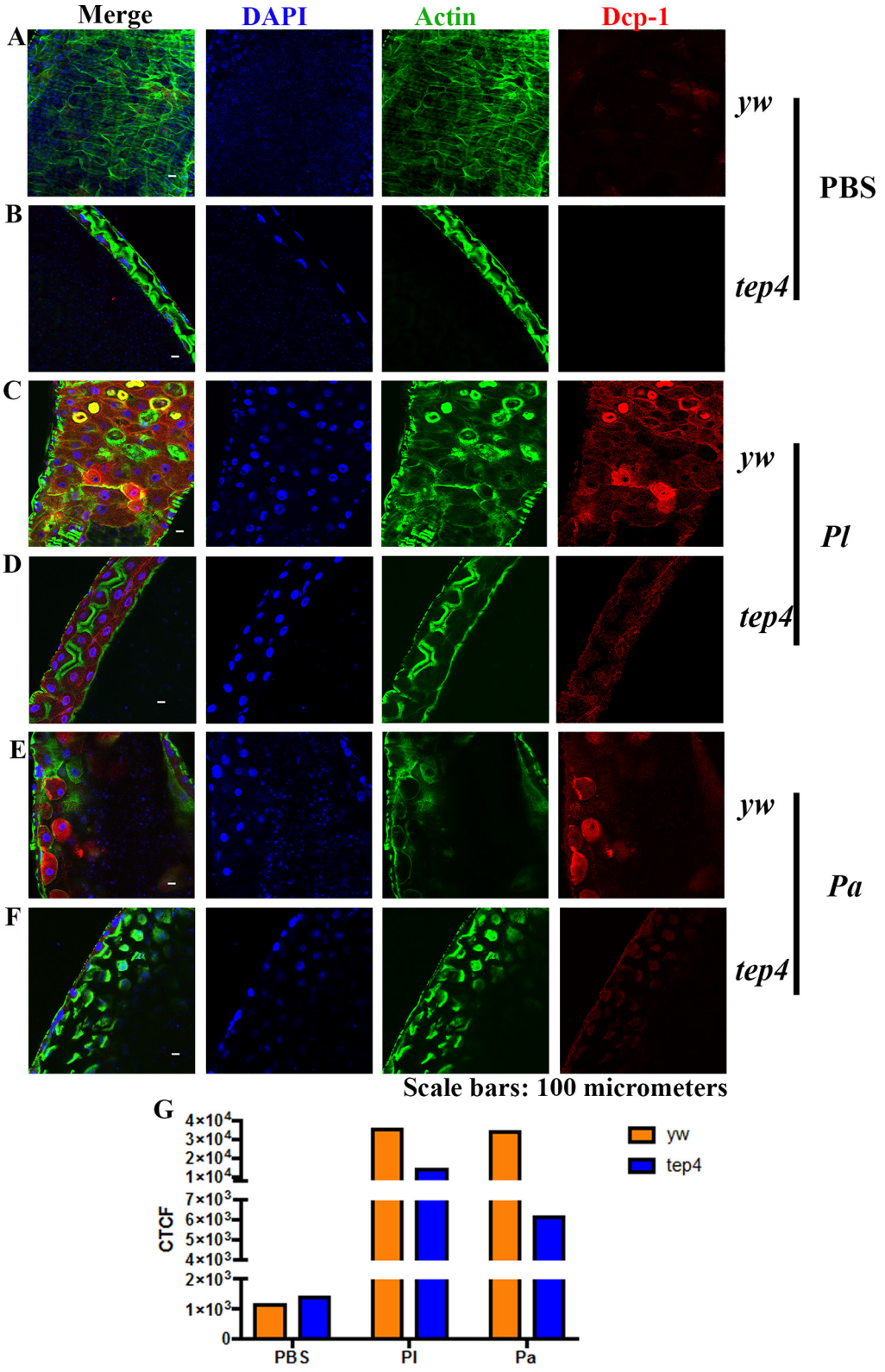

FIG 11 *Drosophila* mutants for *Tep4* display reduced DCP-1 expression in the midgut upon infection with *Photorhabdus*. (A to F) Guts from 7- to 10-day-old *tep4* mutants and background control flies (*yw*) were stained with DCP-1 (red), DAPI (blue), and phalloidin (green). The dissected, stained tissues of flies injected with 1× PBS (A and B), *P. luminescens* (Pl) (C and D), and *P. asymbiotica* (Pa) (E and F) were viewed at a ×40 magnification by using confocal microscopy. (G) Corrected total cell fluorescence (CTCF) was measured to quantify the expression levels of DCP-1 in both background control flies (*yw*) and *tep4* mutant flies by using ImageJ.

increased host survival, lower pathogen burdens, and higher melanization activity in *tep* mutants during the course of *Photorhabdus* infection (11, 35, 54).

In addition to apoptosis, caspases participate in immunity and inflammation (6, 57), and interestingly, sterile inflammation in *Drosophila* can be induced in the absence of pathogens (58). Therefore, *Dronc* upregulation in w^{1118} flies injected with buffer or nonpathogenic *E. coli* bacteria could be the result of wounding. *Photorhabdus* pathogens secrete virulence factors that cause the apoptosis of insect hemocytes and cells in the gut and fat body (17, 59). We showed previously that the inactivation of *Tep2* or *Tep4* increases hemocyte viability in *Photorhabdus*-infected flies (35, 36). Reduced transcript levels of *Dronc*, encoding an apical caspase protein containing a caspase recruitment domain (60), in *tep* mutants signify that these flies undergo less inflammation and cell death during the course of *Photorhabdus* infection. Similarly, reduced expression levels of DCP-1 in the *tep* mutants indicate that these flies undergo less inflammation upon *Photorhabdus* infection. Moreover, as *tep2* and *tep4* mutants contain fewer hemocytes when infected by *P. asymbiotica* (35, 36), they can probably sustain lower levels of inflammation caused by the bacteria. Nitric oxide is capable of acting as both an inducer and an inhibitor of apoptosis by targeting preapoptotic and antiapoptotic molecules, respectively, in mammals as well as in *Drosophila* (61–63). Therefore, an alternative explanation for the increased transcript levels of *Dronc* in the background control flies could be that the inactivation of *Tep2* or *Tep4* may result in elevated levels of nitric oxide that could lead to the inhibition of apoptosis in *Photorhabdus*-infected flies. However, the protective effect of reduced apoptosis probably ceases once nitric oxide levels misbalance the expression of antiapoptotic versus preapoptotic genes, which could result in increased expression levels of proapoptotic genes during the late stages of *Photorhabdus* infection (after 18 hpi) that could consequently increase the survival of *tep* mutant flies.

In conclusion, here, we present evidence that the inactivation of *Tep2* or *Tep4* in *Drosophila* increases the metabolic energy stores of the fly in response to *Photorhabdus* infection. We show that *Tep* gene inactivation reduces numbers of *Photorhabdus* bacteria in the fat body and gut and increases *Dronc* and DCP-1 expression levels as well as nitric oxide production in infected mutants. Our results suggest a novel function of TEP molecules in the interaction of *Drosophila* with the virulent pathogen *Photorhabdus*. Similar research will contribute to a better understanding of the exact function of insect TEP molecules in the host antibacterial immune response and will allow a comprehensive functional comparison with mammalian complement factors.

MATERIALS AND METHODS

Fly strains and bacterial stocks. Loss-of-function *tep2* (f02756, Harvard, and piggyBac) and *tep4* (15936, Bloomington, and p-element) mutants and their background strains (w^{1118} and *yw*) were used in all experiments. All fly strains were fed on instant *Drosophila* medium (Carolina Biological Supply) in deionized water and maintained at 25°C with a 12-h-light/12-h-dark photoperiod.

Photorhabdus luminescens subsp. *laumondii* (strain TT01), *P. asymbiotica* subsp. *asymbiotica* (strain ATCC 43949), and *Escherichia coli* (strain K-12) were used for infections. Bacteria were grown in sterile Luria-Bertani (LB) broth for approximately 18 to 22 h at 30°C on a rotary shaker at 220 rpm. The cultures were pelleted, washed, and resuspended in 1× sterile PBS (Sigma-Aldrich). Bacteria were diluted in 1× PBS to optical densities (ODs) (at 600 nm) of 0.1 for *P. luminescens*, 0.25 for *P. asymbiotica*, and 0.015 for *E. coli* by using a spectrophotometer (NanoDrop 2000c; Thermo Fisher Scientific) (11).

Infection assays. Seven- to ten-day-old adult *Drosophila melanogaster* flies were anesthetized with carbon dioxide and injected intrathoracically with 100 to 300 CFU of each bacterial preparation (*P. luminescens*, *P. asymbiotica*, or *E. coli*) or sterile 1× PBS (septic injury control) by using a Nanoject II apparatus (Drummond Scientific) equipped with glass capillaries prepared with a micropipette puller (Sutter Instruments). Whole flies or gut or fat body tissues were subsequently collected at 6 and 18 hpi and stored at −80°C until further use.

Quantification of trehalose, glycogen, glucose, and triglyceride levels. Adult flies ($n = 5$) were injected with *P. luminescens*, *P. asymbiotica*, *E. coli*, or 1× PBS and collected at 6 and 18 hpi. Groups of flies were washed, and samples were prepared for colorimetric assays of trehalose, glycogen, glucose, and triglyceride, as previously described (25, 64). All samples and standards were run in duplicates, and at least three independent experiments were carried out for each assay. The levels of metabolites were normalized to the total protein content present in the sample.

Lipid droplet staining and quantification. Fat body tissues were dissected in 1× PBS and fixed in 4% paraformaldehyde prepared in 1× PBS for 30 min at room temperature. The tissues were then

TABLE 1 List of primers used in this study[a]

Gene	GenBank accession no.	Primer direction	Primer sequence (5′–3′)	T_m (°C)
RpL32	CG7939	Forward	GATGACCATCCGCCCAGCA	61
		Reverse	CGGACCGACAGCTGCTTGGC	
Pl16s	KC237383	Forward	ACAGAGTTGGATCTTGACGTTACCC	61
		Reverse	AATCTTGTTTGCTCCCCACGCTT	
Dronc	CG8091	Forward	AGCTTGCTAACGCAGGGTC	61
		Reverse	CCTTTATCTCGCTAAACGAACGG	
Tep2	CG7052	Forward	CGTTCTGCTGGCTTTCTTC	52.5
		Reverse	ATACTGGTCGTCCGTCTTGTC	
Tep4	CG10363	Forward	GCTGCAGAACCAGATCGAAATC	61
		Reverse	ATGACTTTGGCGACGTCTTGAT	

[a]T_m, melting temperature.

washed twice in 1× PBS and stained with a 1:1,000 dilution of 0.05% Nile Red-O in 1 mg/ml methanol for 30 min in the dark. Tissues were mounted in Vectashield (catalog number H1200; Vector Laboratories), and images were taken by using an Olympus confocal microscope. To quantify lipid droplet sizes, the area of the 15 largest lipid droplets per fat body was measured by using Image J. This was repeated for at least three independent samples for each fly strain.

RNA isolation, gene transcript levels, and bacterial loads. RNA was isolated from frozen flies ($n = 5$) or gut or fat body tissues by using the PrepEase RNA spin kit (Affymetrix USB) or TRIzol reagent (Ambion, Thermo Fisher Scientific) according to the manufacturers' protocols. RNA samples were adjusted to 350 ng for cDNA synthesis (Applied Biosystems, Thermo Fisher Scientific). Quantitative reverse transcription-PCR (qRT-PCR) was performed by using the CFX96 Touch real-time PCR detection system (Bio-Rad), and the $\Delta\Delta C_T$ method was used for analysis of results (11). Data are presented as the ratio of injected flies to untreated flies (baseline controls), as previously described (11). A list of primers used for the qRT-PCR assays is shown in Table 1.

To estimate bacterial loads, standard curves were generated for each bacterial strain by using primers to amplify their 16S rRNA genes, as described previously (12). qPCR was performed on bacterial cDNA samples, as described above. Numbers of CFU were determined from the standard curves. All experiments were performed at least three times.

Nitric oxide estimation. Equal numbers ($n = 4$) of male and female adult flies were homogenized in 1× PBS at 6 and 18 hpi. Following centrifugation at 10,000 × *g* for 10 min at 4°C, the supernatants were collected and mixed with Griess reagent at a 1:1 ratio (Sigma-Aldrich). Following incubation for 15 min at room temperature, the absorbance (595 nm) was measured by using a spectrophotometer (NanoDrop 2000c). A silver nitrite standard curve was constructed to estimate the concentration of nitrite in the samples. Nitric oxide levels are represented as the concentration of nitrite normalized to the total protein content, and the experiments were performed at least three times.

Gut staining and fluorescence quantification. Guts from infected or uninfected 7- to 10-day-old adult flies were dissected in 1× PBS, as mentioned above. Gut tissues were fixed for 30 min in 4% paraformaldehyde in PBST (PBS plus 0.3% Triton). After two washes in PBST, guts were treated with a 1:100 dilution of Dcp-1 primary antibody (Cell Signaling Technology) in PBST at 4°C overnight. Following two washes, the tissues were blocked for 2 h in PBSTB (PBST plus 0.1% bovine serum albumin). Rinsing was done twice in PBST, and tissues were incubated with a 1:500 dilution of Alexa Fluor 544 anti-rabbit secondary antibody for 2 h at room temperature. After two washes, tissues were finally incubated with phalloidin-actin for 20 min before being mounted in Vectashield mounting medium (catalog number H1200; Vector Laboratories). Images were taken by using an Olympus confocal microscope.

Images were first converted into 16-bit gray scale images, and three random areas of DCP-1 expression were used for quantification. Relative amounts of fluorescence were measured with ImageJ software by using Shanbhag thresholding on images and calculating the resulting area, integrated density, and mean fluorescence of the background. The following equation was used: corrected total fluorescence = integrated density − (area × mean fluorescence of background).

Statistical analysis. All statistical analyses were performed by using GraphPad Prism7 software. For gene transcript levels, nitric oxide quantification, and metabolic activity measurements, data were analyzed by using two-way analysis of variance (ANOVA) with a Tukey *post hoc* test for multiple comparisons. For bacterial load estimations, samples were analyzed by using a two-tailed *t* test. *P* values of <0.05 were considered statistically significant.

ACKNOWLEDGMENTS

We thank members of the Department of Biological Sciences at GWU for critical reading of the manuscript.

This research was supported by a start-up fund from the Columbian College of Arts

and Sciences at GWU to I.E. and by Harlan summer fellowships from the Department of Biological Sciences at GWU and a scholarship from the Cosmos Club Foundation (Washington, DC) to U.S. The I.E. laboratory is funded by the National Institutes of Health (grant 1R01AI110675-01A1).

REFERENCES

1. Shirasu-Hiza MM, Schneider DS. 2007. Confronting physiology: how do infected flies die? Cell Microbiol 9:2775–2783. https://doi.org/10.1111/j.1462-5822.2007.01042.x.
2. Apidianakis Y, Rahme LG. 2009. *Drosophila melanogaster* as a model host for studying *Pseudomonas aeruginosa* infection. Nat Protoc 4:1285–1294. https://doi.org/10.1038/nprot.2009.124.
3. Razzell W, Wood W, Martin P. 2011. Swatting flies: modelling wound healing and inflammation in *Drosophila*. Dis Model Mech 4:569–574. https://doi.org/10.1242/dmm.006825.
4. Nehme NT, Liegeois S, Kele B, Giammarinaro P, Pradel E, Hoffmann JA, Ewbank JJ, Ferrandon D. 2007. A model of bacterial intestinal infections in *Drosophila melanogaster*. PLoS Pathog 3:e173. https://doi.org/10.1371/journal.ppat.0030173.
5. Arnold PA, Johnson KN, White CR. 2013. Physiological and metabolic consequences of viral infection in *Drosophila melanogaster*. J Exp Biol 216:3350–3357. https://doi.org/10.1242/jeb.088138.
6. Lemaitre B, Hoffmann J. 2007. The host defense of *Drosophila melanogaster*. Annu Rev Immunol 25:697–743. https://doi.org/10.1146/annurev.immunol.25.022106.141615.
7. Dionne M. 2014. Immune-metabolic interaction in *Drosophila*. Fly (Austin) 8:75–79. https://doi.org/10.4161/fly.28113.
8. Ayres JS, Schneider DS. 2009. The role of anorexia in resistance and tolerance to infections in *Drosophila*. PLoS Biol 7:e1000150. https://doi.org/10.1371/journal.pbio.1000150.
9. Chambers MC, Song KH, Schneider DS. 2012. *Listeria monocytogenes* infection causes metabolic shifts in *Drosophila melanogaster*. PLoS One 7:e50679. https://doi.org/10.1371/journal.pone.0050679.
10. Castillo JC, Shokal U, Eleftherianos I. 2013. Immune gene transcription in *Drosophila* adult flies infected by entomopathogenic nematodes and their mutualistic bacteria. J Insect Physiol 59:179–185. https://doi.org/10.1016/j.jinsphys.2012.08.003.
11. Shokal U, Eleftherianos I. 2017. Thioester-containing protein-4 regulates the *Drosophila* immune signaling and function against the pathogen Photorhabdus. J Innate Immun 9:83–93. https://doi.org/10.1159/000450610.
12. Shokal U, Yadav S, Atri J, Accetta J, Kenney E, Banks K, Katakam A, Jaenike J, Eleftherianos I. 2016. Effects of co-occurring *Wolbachia* and *Spiroplasma* endosymbionts on the *Drosophila* immune response against insect pathogenic and non-pathogenic bacteria. BMC Microbiol 16:16. https://doi.org/10.1186/s12866-016-0634-6.
13. Castillo JC, Creasy T, Kumari P, Shetty A, Shokal U, Tallon LJ, Eleftherianos I. 2015. *Drosophila* anti-nematode and antibacterial immune regulators revealed by RNA-Seq. BMC Genomics 16:519. https://doi.org/10.1186/s12864-015-1690-2.
14. Waterfield NR, Ciche T, Clarke D. 2009. *Photorhabdus* and a host of hosts. Annu Rev Microbiol 63:557–574. https://doi.org/10.1146/annurev.micro.091208.073507.
15. Ciche TA, Ensign JC. 2003. For the insect pathogen *Photorhabdus luminescens*, which end of a nematode is out? Appl Environ Microbiol 69:1890–1897. https://doi.org/10.1128/AEM.69.4.1890-1897.2003.
16. ffrench-Constant RH, Dowling A, Waterfield NR. 2007. Insecticidal toxins from *Photorhabdus* bacteria and their potential use in agriculture. Toxicon 49:436–451. https://doi.org/10.1016/j.toxicon.2006.11.019.
17. Eleftherianos I, ffrench-Constant RH, Clarke DJ, Dowling AJ, Reynolds SE. 2010. Dissecting the immune response to the entomopathogen *Photorhabdus*. Trends Microbiol 18:552–560. https://doi.org/10.1016/j.tim.2010.09.006.
18. Silva CP, Waterfield NR, Daborn PJ, Dean P, Chilver T, Au CP, Sharma S, Potter U, Reynolds SE, ffrench-Constant RH. 2002. Bacterial infection of a model insect: *Photorhabdus luminescens* and *Manduca sexta*. Cell Microbiol 4:329–339. https://doi.org/10.1046/j.1462-5822.2002.00194.x.
19. Daborn PJ, Waterfield N, Silva CP, Au CP, Sharma S, ffrench-Constant RH. 2002. A single *Photorhabdus* gene, *makes caterpillars floppy* (*mcf*), allows *Escherichia coli* to persist within and kill insects. Proc Natl Acad Sci U S A 99:10742–10747. https://doi.org/10.1073/pnas.102068099.
20. Lang AE, Schmidt G, Schlosser A, Hey TD, Larrinua IM, Sheets JJ, Mannherz HG, Aktories K. 2010. *Photorhabdus luminescens* toxins ADP-ribosylate actin and RhoA to force actin clustering. Science 327:1139–1142. https://doi.org/10.1126/science.1184557.
21. Blackburn M, Golubeva E, Bowen D, ffrench-Constant RH. 1998. A novel insecticidal toxin from *Photorhabdus luminescens*, toxin complex a (Tca), and its histopathological effects on the midgut of *Manduca sexta*. Appl Environ Microbiol 64:3036–3041.
22. Eleftherianos I, Boundy S, Joyce SA, Aslam S, Marshall JW, Cox RJ, Simpson TJ, Clarke DJ, ffrench-Constant RH, Reynolds SE. 2007. An antibiotic produced by an insect-pathogenic bacterium suppresses host defenses through phenoloxidase inhibition. Proc Natl Acad Sci U S A 104:2419–2424. https://doi.org/10.1073/pnas.0610525104.
23. Eleftherianos I, Waterfield NR, Bone P, Boundy S, ffrench-Constant RH, Reynolds SE. 2009. A single locus from the entomopathogenic bacterium *Photorhabdus luminescens* inhibits activated *Manduca sexta* phenoloxidase. FEMS Microbiol Lett 293:170–176. https://doi.org/10.1111/j.1574-6968.2009.01523.x.
24. Hu K, Webster JM. 2000. Antibiotic production in relation to bacterial growth and nematode development in *Photorhabdus-Heterorhabditis* infected *Galleria mellonella* larvae. FEMS Microbiol Lett 189:219–223. https://doi.org/10.1111/j.1574-6968.2000.tb09234.x.
25. McCormack S, Yadav S, Shokal U, Kenney E, Cooper D, Eleftherianos I. 2016. The insulin receptor substrate Chico regulates antibacterial immune function in *Drosophila*. Immun Ageing 13:15. https://doi.org/10.1186/s12979-016-0072-1.
26. Christophides GK, Vlachou D, Kafatos FC. 2004. Comparative and functional genomics of the innate immune system in the malaria vector *Anopheles gambiae*. Immunol Rev 198:127–148. https://doi.org/10.1111/j.0105-2896.2004.0127.x.
27. Markiewski MM, Lambris JD. 2007. The role of complement in inflammatory diseases from behind the scenes into the spotlight. Am J Pathol 171:715–727. https://doi.org/10.2353/ajpath.2007.070166.
28. Shokal U, Eleftherianos I. 2017. Evolution and function of thioester-containing proteins and the complement system in the innate immune response. Front Immunol 8:759. https://doi.org/10.3389/fimmu.2017.00759.
29. Blandin SA, Marois E, Levashina EA. 2008. Antimalarial responses in *Anopheles gambiae*: from a complement-like protein to a complement-like pathway. Cell Host Microbe 3:364–374. https://doi.org/10.1016/j.chom.2008.05.007.
30. Fraiture M, Baxter RH, Steinert S, Chelliah Y, Frolet C, Quispe-Tintaya W, Hoffmann JA, Blandin SA, Levashina EA. 2009. Two mosquito LRR proteins function as complement control factors in the TEP1-mediated killing of *Plasmodium*. Cell Host Microbe 5:273–284. https://doi.org/10.1016/j.chom.2009.01.005.
31. Bou Aoun R, Hetru C, Troxler L, Doucet D, Ferrandon D, Matt N. 2011. Analysis of thioester-containing proteins during the innate immune response of *Drosophila melanogaster*. J Innate Immun 3:52–64. https://doi.org/10.1159/000321554.
32. Lagueux M, Perrodou E, Levashina EA, Capovilla M, Hoffmann JA. 2000. Constitutive expression of a complement-like protein in Toll and JAK gain-of-function mutants of *Drosophila*. Proc Natl Acad Sci U S A 97:11427–11432. https://doi.org/10.1073/pnas.97.21.11427.
33. Stroschein-Stevenson SL, Foley E, O'Farrell PH, Johnson AD. 2006. Identification of *Drosophila* gene products required for phagocytosis of *Candida albicans*. PLoS Biol 4:e4. https://doi.org/10.1371/journal.pbio.0040004.
34. Dostalova A, Rommelaere S, Poidevin M, Lemaitre B. 2017. Thioester-containing proteins regulate the Toll pathway and play a role in *Drosophila* defence against microbial pathogens and parasitoid wasps. BMC Biol 15:79. https://doi.org/10.1186/s12915-017-0408-0.
35. Shokal U, Kopydlowski H, Eleftherianos I. 2 June 2017. The distinct function of Tep2 and Tep6 in the immune defense of *Drosophila melanogaster* against the pathogen *Photorhabdus*. Virulence https://doi.org/10.1080/21505594.2017.1330240.

36. Shokal U, Eleftherianos I. 2017. The *Drosophila* thioester containing protein-4 participates in the induction of the cellular immune response to the pathogen *Photorhabdus*. Dev Comp Immunol 76:200–208. https://doi.org/10.1016/j.dci.2017.06.008.
37. Dionne MS, Pham LN, Shirasu-Hiza M, Schneider DS. 2006. Akt and FOXO dysregulation contribute to infection-induced wasting in *Drosophila*. Curr Biol 16:1977–1985. https://doi.org/10.1016/j.cub.2006.08.052.
38. Yasugi T, Yamada T, Nishimura T. 2017. Adaptation to dietary conditions by trehalose metabolism in *Drosophila*. Sci Rep 7:1619. https://doi.org/10.1038/s41598-017-01754-9.
39. Chtarbanova S, Lamiable O, Lee KZ, Galiana D, Troxler L, Meignin C, Hetru C, Hoffmann JA, Daeffler L, Imler JL. 2014. *Drosophila* C virus systemic infection leads to intestinal obstruction. J Virol 88:14057–14069. https://doi.org/10.1128/JVI.02320-14.
40. Anand P, Cermelli S, Li Z, Kassan A, Bosch M, Sigua R, Huang L, Ouellette AJ, Pol A, Welte MA, Gross SP. 2012. A novel role for lipid droplets in the organismal antibacterial response. eLife 1:e00003. https://doi.org/10.7554/eLife.00003.
41. Rynes J, Donohoe CD, Frommolt P, Brodesser S, Jindra M, Uhlirova M. 2012. Activating transcription factor 3 regulates immune and metabolic homeostasis. Mol Cell Biol 32:3949–3962. https://doi.org/10.1128/MCB.00429-12.
42. Ajjuri RR, O'Donnell JM. 4 December 2013. Novel whole-tissue quantitative assay of nitric oxide levels in *Drosophila* neuroinflammatory response. J Vis Exp https://doi.org/10.3791/50892.
43. Meier P, Silke J, Leevers SJ, Evan GI. 2000. The *Drosophila* caspase DRONC is regulated by DIAP1. EMBO J 19:598–611. https://doi.org/10.1093/emboj/19.4.598.
44. Kondo S, Senoo-Matsuda N, Hiromi Y, Miura M. 2006. DRONC coordinates cell death and compensatory proliferation. Mol Cell Biol 26:7258–7268. https://doi.org/10.1128/MCB.00183-06.
45. Ganeshan K, Chawla A. 2014. Metabolic regulation of immune responses. Annu Rev Immunol 32:609–634. https://doi.org/10.1146/annurev-immunol-032713-120236.
46. DiAngelo JR, Bland ML, Bambina S, Cherry S, Birnbaum MJ. 2009. The immune response attenuates growth and nutrient storage in *Drosophila* by reducing insulin signaling. Proc Natl Acad Sci U S A 106:20853–20858. https://doi.org/10.1073/pnas.0906749106.
47. Erkosar B, Defaye A, Bozonnet N, Puthier D, Royet J, Leulier F. 2014. *Drosophila* microbiota modulates host metabolic gene expression via IMD/NF-kappaB signaling. PLoS One 9:e94729. https://doi.org/10.1371/journal.pone.0094729.
48. Hand SC, Hardewig I. 1996. Downregulation of cellular metabolism during environmental stress: mechanisms and implications. Annu Rev Physiol 58:539–563. https://doi.org/10.1146/annurev.ph.58.030196.002543.
49. Barletta AB, Alves LR, Silva MC, Sim S, Dimopoulos G, Liechocki S, Maya-Monteiro CM, Sorgine MH. 2016. Emerging role of lipid droplets in *Aedes aegypti* immune response against bacteria and dengue virus. Sci Rep 6:19928. https://doi.org/10.1038/srep19928.
50. Bozza PT, Magalhaes KG, Weller PF. 2009. Leukocyte lipid bodies—biogenesis and functions in inflammation. Biochim Biophys Acta 1791:540–551. https://doi.org/10.1016/j.bbalip.2009.01.005.
51. Ferrandon D, Imler JL, Hetru C, Hoffmann JA. 2007. The *Drosophila* systemic immune response: sensing and signalling during bacterial and fungal infections. Nat Rev Immunol 7:862–874. https://doi.org/10.1038/nri2194.
52. Capo F, Charroux B, Royet J. 2016. Bacteria sensing mechanisms in *Drosophila* gut: local and systemic consequences. Dev Comp Immunol 64:11–21. https://doi.org/10.1016/j.dci.2016.01.001.
53. Hallem EA, Rengarajan M, Ciche TA, Sternberg PW. 2007. Nematodes, bacteria, and flies: a tripartite model for nematode parasitism. Curr Biol 17:898–904. https://doi.org/10.1016/j.cub.2007.04.027.
54. Foley E, O'Farrell PH. 2003. Nitric oxide contributes to induction of innate immune responses to gram-negative bacteria in *Drosophila*. Genes Dev 17:115–125. https://doi.org/10.1101/gad.1018503.
55. Arefin B, Kucerova L, Krautz R, Kranenburg H, Parvin F, Theopold U. 2015. Apoptosis in hemocytes induces a shift in effector mechanisms in the *Drosophila* immune system and leads to a pro-inflammatory state. PLoS One 10:e0136593. https://doi.org/10.1371/journal.pone.0136593.
56. Kraaijeveld AR, Elrayes NP, Schuppe H, Newland PL. 2011. L-Arginine enhances immunity to parasitoids in *Drosophila melanogaster* and increases NO production in lamellocytes. Dev Comp Immunol 35:857–864. https://doi.org/10.1016/j.dci.2011.03.019.
57. Shalini S, Dorstyn L, Dawar S, Kumar S. 2015. Old, new and emerging functions of caspases. Cell Death Differ 22:526–539. https://doi.org/10.1038/cdd.2014.216.
58. Shaukat Z, Liu D, Gregory S. 2015. Sterile inflammation in *Drosophila*. Mediators Inflamm 2015:369286. https://doi.org/10.1155/2015/369286.
59. Costa SC, Girard PA, Brehelin M, Zumbihl R. 2009. The emerging human pathogen *Photorhabdus asymbiotica* is a facultative intracellular bacterium and induces apoptosis of macrophage-like cells. Infect Immun 77:1022–1030. https://doi.org/10.1128/IAI.01064-08.
60. Daish TJ, Mills K, Kumar S. 2004. *Drosophila* caspase DRONC is required for specific developmental cell death pathways and stress-induced apoptosis. Dev Cell 7:909–915. https://doi.org/10.1016/j.devcel.2004.09.018.
61. Brune B, von Knethen A, Sandau KB. 1999. Nitric oxide (NO): an effector of apoptosis. Cell Death Differ 6:969–975. https://doi.org/10.1038/sj.cdd.4400582.
62. Dzhansugurova LB. 2011. Effect of nitric oxide on expression of apoptotic genes and HSP70 in *Drosophila*. Ontogenez 42:425–438. (In Russian.)
63. Tejedo JR, Tapia-Limonchi R, Mora-Castilla S, Cahuana GM, Hmadcha A, Martin F, Bedoya FJ, Soria B. 2010. Low concentrations of nitric oxide delay the differentiation of embryonic stem cells and promote their survival. Cell Death Dis 1:e80. https://doi.org/10.1038/cddis.2010.57.
64. Tennessen JM, Barry WE, Cox J, Thummel CS. 2014. Methods for studying metabolism in *Drosophila*. Methods 68:105–115. https://doi.org/10.1016/j.ymeth.2014.02.034.